Research Article

BIOMEDICAL Journal of Scientific & Technical Research

ISSN: 2574 -1241

DOI: 10.26717/BJSTR.2020.28.004701

Influence of Surfactants on The Optical Properties of WO_3 Nanoparticles Synthesis by Precipitation Method

Fawzi S Kodeh[1]* and Talaat M Hammad[2]

[1]*Chemistry Department, Faculty of Science, Al-Azhar University, Palestine*

[2]*Physics Department, Faculty of Science, Al-Azhar University, Palestine*

***Corresponding author:** Fawzi S Kodeh, Chemistry Department, Faculty of Science, Al-Azhar University, P.O. Box 1277, Gaza, Palestine

ARTICLE INFO

Received: June 28, 2020

Published: July 09, 2020

Citation: Fawzi S Kodeh, Talaat M Hammad. Influence of Surfactants on The Optical Properties of WO_3 Nanoparticles Synthesis by Precipitation Method. Biomed J Sci & Tech Res 28(5)-2020. BJSTR. MS.ID.004701.

Keywords: Nanoparticles; WO_3; Surfactants; Optical Properties

ABSTRACT

Tungsten trioxide (WO_3) nanostructures have been synthesized with sodium tungstate dihydrate (Na_2WO_4-$2H_2O$) additives Ceteareth-25 and alkyl hydroxyl ethyl dimethyl ammonium chloride (HY) surfactants using precipitation process. For the structural investigations of the samples, X-ray Diffraction Technique (XRD) and scanning electron microscopy (TEM). Optical features of samples were studied by UV-vis absorption and photoluminescence (PL).X–ray analysis shows that hexagonal WO_3 nanoparticles are formed. The mean particle Size of samplesbetween10-17nm. The presence of cationic HY surfactant reduced the particle size of the samples. The absorption spectra of WO_3/HY showed a blue shift, while the spectra of WO_3/ Cet. showed a red shift. PL spectra of pure WO_3, WO_3/ Ceteareth-25 and WO_3/HY nanoparticles showed ultraviolet emissions (369, 373 and 354nm) and red emissions (624nm).

Abbreviations: XRD: X-ray Diffraction Technique; CPYB: Cetylpyridinium Bromide; HTAC: Hexadecyl Trimethyl Ammonium Bromide; TTAB: Tetradecyl Trimethyl Ammonium Bromide; SEM: Scanning Electron Microscopy; FWHM: Full Width at Half Maximum

Introduction

In many fields of chemistry, physics and material science, metal oxides play a very important role [1-6]. The metal elements are capable to make a huge sort of oxide compounds [7]. These can receive countless basic geometry with an electronic structure, which will show metallic, semiconductor or insulator character. Oxides are used in the manufacture of microelectronic circuits, sensors, piezoelectrical devices, fuel cells, surface passivation coating against corrosion and in technological applications ascatalysts. Within the emerging field of nanotechnology, the objective is to create nanostructures or nanoarrays with unique properties that are appreciated by large or single particle species [8-12]. Because of dimension their small and high density of corner or edge surface sites, oxide nanoparticles can show specific physical and chemical properties. Tungsten oxide (WO_3) may be well known n-type wide band gap semiconductor, inexpensive, environmentally friendly and chemically stable [13-15] among the prevailing metal- oxide semiconductors. Tungsten oxide has been investigated for photo catalysts thanks to their fantastic electrochromic, gaschromic and optochromic properties [16]. Its other unique properties have additionally been explored in flat panel displays [17], optoelectronics [18], energy devices [19] and gas sensors [20].

In recent years, due to photochromic effect, WO_3 based materials have been utilized in clinical and natural examination as antibacterial coatings, biosensors, the ranostic materials, and materials for proliferation control [21]. Various methods are made to organize WO_3 nano-particles like template assisted growth [22], anodization [23], conventional thermal evaporation [24], hot wall chemical vapor deposition [25], arc discharge [26], pulsed laser deposition [27], hydrothermal method [28] and solvothermal method [29]. Previous studies are conducted to synthesize WO3 nanoparticles. Priya et al. prepared WO_3 by using precipitation method within the presence of surfactants CTAB and PEG- 600

[30]. Hariharan et al. synthesized WO_3 nanoparticles using EDTA as a surfactant by simple household microwave irradiation technique [31]. However, in another study, WO3 nanoparticles were synthesized by facile solution procedure using different cationic surfactants [32]. Abdul Razaket et al. synthesized WO_3 nanoparticles with CTAB surfactant assisting the hydrothermal method [33]. Zhang et al. have correctly developed monoclinic WO_3 nanoplates via a topochemical conversion manner through one-step template-free hydrothermal route. The results showed that

WO_3 nanoplates are approximately 100–170 nm long and 30–50nm thick [34]. Another researcher developed WO_3 square nanoplates using natural acids specifically L (+)-tartaric acid and acid as assistant agents [35]. Hexagonal WO_3 phase used to be determined in the presence of hydroxy acid with particle size ~200nm and thickness ~100nm, whereas orthorhombic phase was once came about in the presence of acid with average particle length ~500nm and thickness ~100nm, respectively. The SAED pattern suggests that the pure WO_3 square nanoplates are single crystalline. The precipitation technique among these methods is reasonable, easy and yields small particle size, excessive homogeneity, and stoichiometry that could not be performed at high temperatures. Ahmad Umar et al. used different cationic surfactants with various chain lengths eg., Cetylpyridinium Chloride (CPyC), Cetylpyridinium Bromide (CPyB), Hexadecyltrimethyl Ammonium Bromide (HTAC) and Tetradecyl trimethyl Ammonium Bromide (TTAB) were utilized.

These serve as double need: initially, functionalization of the nanoparticles beside controling the stoichiometry, subsequently preventing the agglomeration in the nanoparticles [36]. The use of different types of surfactants offers the potential to accumulate control over the WO_3 nanoparticle measurement, morphology and size distribution, which is essential for customizing optical, electrical, chemical, and magnetic properties of nanoparticles for special applications [37-38]. To our knowledge, however, tungsten oxide nanoparticles are synthesized using a chemical method of co-precipitation within the presence of nonionic Ceteareth-25 (polyoxyethylene ether of higher saturated fatty alcohols) and cationic HY surfactants and their optical properties were presented for the first time during this study.

Experimental

Reagents

Sodium tungstate dihydrate ($Na_2WO_4 \cdot 2H_2O$) oxalic acid, HCL from MERCK(Darmatadt, Germany), alkyl hydroxyethyl dimethyl ammonium chloride surfactant $C_{16}H_{36}NOCl$, $C_{18}H_{40}NOCl$ (praepagen HY, R = 12–14) were purchased from Clarian and used as received, Ceteareth-25 surfactant (polyoxyethylene 25 cetyl ether, C16H33(OCH2CH2)25-OH) from Sigma aldersh.

Spectra

UV-vis absorption spectra were obtained using a UV -3101PC spectrophotometer (Shimadzu, UV-VIS-NIR scaning spectrophotometer) between 200 and 700nm in the wavelength range. A spectrofluorometer (JASCO, FP6500) was used to record PL spectra; the wavelength of extinction was 300 nm.

SEM and X-ray Diffraction (XRD)

The X-ray diffraction pattern (XRD) of the dried as prepared and labeled samples was obtained using a PANalytical X0 pert (PANalytical) X-ray diffractometer with a wavelength of Cu Ka 154nm below 40kV and 200mA. The morphological studies of prepared nanoparticles were studied by Scanning Electron Microscopy (SEM) with a Philips X130 ESEMFEG.

Synthesis

WO_3 nanoparticles were synthesized by dissolving sodium tungstate dihydrate ($Na_2WO_4 \cdot 2H_2O$) in 20ml deionized water solution. The solution was diluted separately with oxalic acid (1M), (1g) and hydrochloric acid 1M (HCL), diluted with deionized water, and stirred in a precursor solution. The final product solution is heated to 60°C for 1 hour to ensure complete reaction. White and green yellow precipitate was obtained in the presence of surfactant, then washed several times with de-ionized water and ethanol. Finally, the precipitate powder was collected and dried in an oven at 600°C for 6 hours. Samples were placed in a muffle furnace at 4000C for 1 hour to ensure the crystallization of WO_3, WO_3/ HY and WO_3/ Ceteareth-25 nanoparticles.

Result and Discussion

Figure 1 shows the XRD pattern of the WO_3 nanoparticles prepared with and without surfactant solutions. From both samples, the XRD spectra show diffraction peaks(2θ) at angles of 14o, 22.9°, 24.5°, 27.2°,28. 3°, 33.6°, 36. 7°, 42.89°, 46.77°, 49.08°, 50.04°, 52.19°, 55.61°, 58.26°, 63.55° that can be attributed to the (100), (001), (110), (200), (111), (201), (300), (211), (102), (220), (310), (202), (400), (401) and (523) planes, respectively. These peaks matched very well with the hexagonal phase of the WO3 nanostructure with the lattice constants a = 7.298 Å, c = 3.899 Å (JCPDS 33-1387). No obvious peaks of other phases are detected, indicating that the product is mainly composed of hexagonal WO_3. Strong and sharp diffraction peaks additionally indicate a proper crystallinity of the sample. The average particle sizes of the samples were estimated by using the Debye–Scherrer equation

$$D=\frac{k\lambda}{(B\cos\theta)} \quad (1)$$

where D is the particle size, k a fixed number of 0.9, λ the X-ray wavelength, θ the Bragg's angle in radians, and B the full width at

half maximum of the peak in radians.It should be noted here that the Full Width At Half Maximum (FWHM) of the diffraction peaks changes with various additives of surfactants. Furthermore, the crystalline size can be estimated to be 15, 17 and 10nm, for pure WO_3, WO_3/ Ceteareth-25 and WO_3/HY nanoparticles respectively. On the other hand, in case of HY, the WO_3 nanoparticles show smaller crystalline size of 10nm. SEM analyzed the morphology of the WO_3 samples. (Figure 2a & 2b) shows some SEM micrographs of WO_3 and WO_3/ Ceteareth-25, and WO_3/HY nanoparticles. Figure 2 shows the surface morphologies of all samples, which have agglomerated irregular particle structure. Obviously, the WO3 nanoparticles have grainy shapes and tend to form aggregations. The optical measurement of the prepared sample was performed at room temperature by using UV–visible absorbance spectrophotometer. The recorded absorbance spectra of WO_3, WO_3/ Ceteareth-25, WO_3/ HY nanoparticles are shown in (Figure 3). The absorption peak corresponding to WO_3, WO_3/ Ceteareth-25, WO_3/HY nanoparticles samples are obtained at 303, 306 and 300 nm, respectively (Figure 3). Absorption is generallydependent on several parameters, such as band gap differences and Impurity centers [39]. The optical band gap samples can be calculated using the Tauc equation that shows a relationship between the photon energy incident of semiconductors and the absorption coefficient [40]:

$$(\alpha hv) = B\left(hv - E_g\right)^{\frac{1}{2}} \quad (2)$$

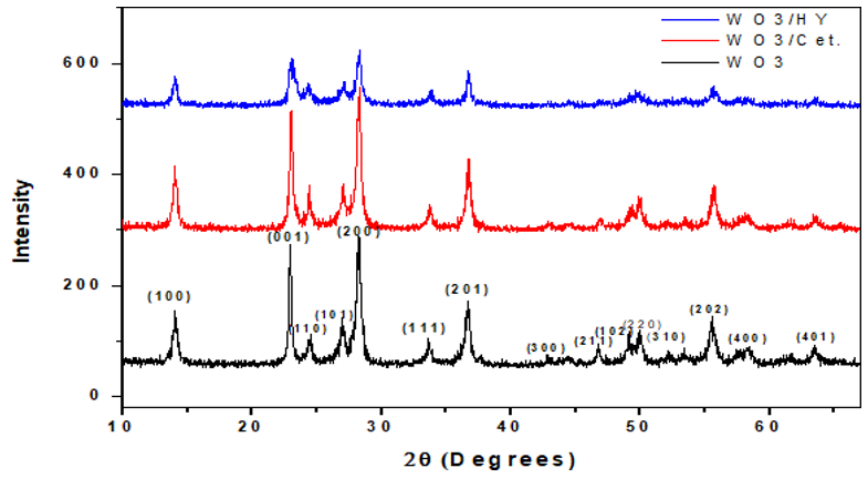

Figure 1: XRD pattern of the pure WO_3, WO_3/ Ceteareth-25 and WO_3/HY nanoparticles.

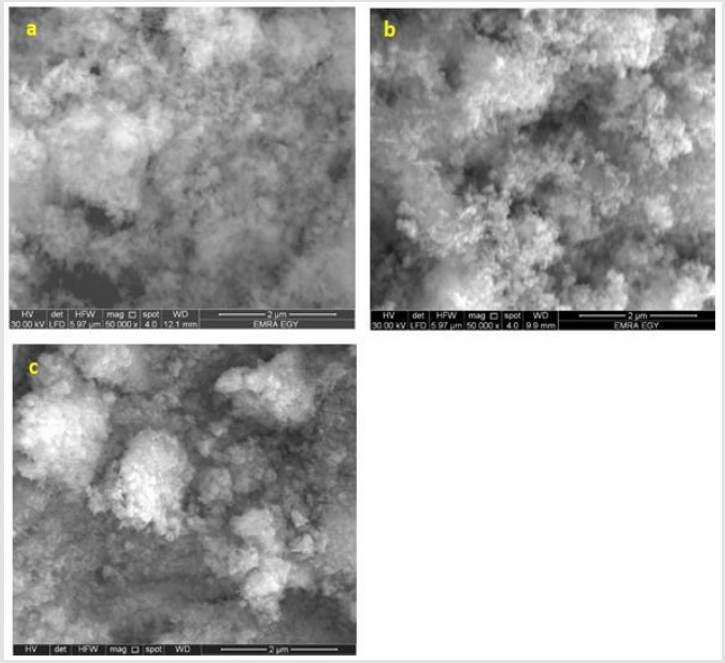

Figure 2: SEM micrographs of WO_3 and WO_3/Ceteareth-25, and WO_3/HY nanoparticles.

DOI: 10.26717/BJSTR.2020.28.004701

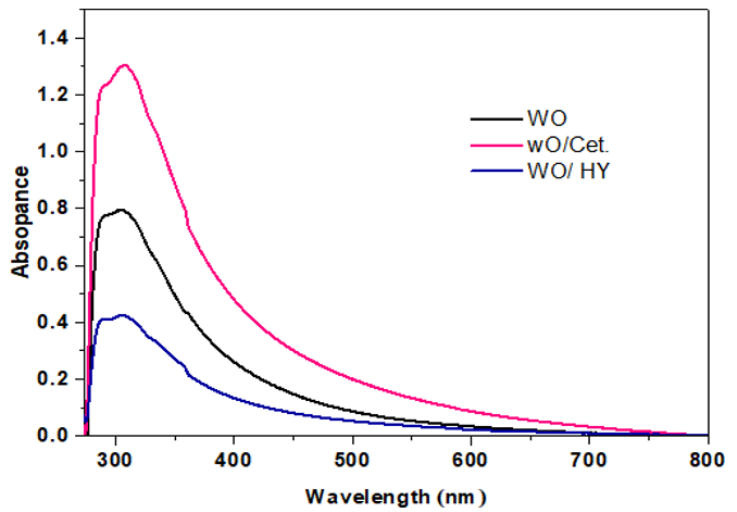

Figure 3: UV-vis spectra of WO_3 and WO_3/ Ceteareth-25, and WO_3/HY nanoparticles.

Where B is the constant and Eg is the band gap energy of the material. The energy band gap (Eg) of sample can be found by plotting $(\alpha h\nu)^2$ versus hν and extrapolating the linear portion of the absorption edge as shown in Figure 4 Band gaps 3.19, 3.23, and 3.26 eV were obtained for these samples, respectively. These values offer an good agreement with the reported value [38]. A significant blue shift in excitonic absorption compared to that of the WO_3 nanoparticles for nanoparticles prepared in the presence of surfactant HY. The prepared nanoparticles in aqueous solution of various cationic surfactants have different dimensional parameters, and this is quite evident from their spectrum, which demonstrates thesize dependence of the absorption spectrum arising from the quantum confinement of photo-generated electron-hole pairs [32]. PLspectro- scopy is a useful study to measure the energy distribution of photons emitted after optical excitati on and to understand the pair of electron hole in semiconductor oxide materials [41]. The spectra of photoluminescence can be used to analyze WO_3 samples, oxygen vacancy and lattice distortion as shown in the (Figure 5). The spectra were recorded under the excitation wavelength of 300nm at room temperature. Both pure WO_3, WO_3 / Ceteareth-25 and WO_3/HY nanoparticles show ultraviolet emissions (369, 373 and 354nm) and redemissions (624nm).

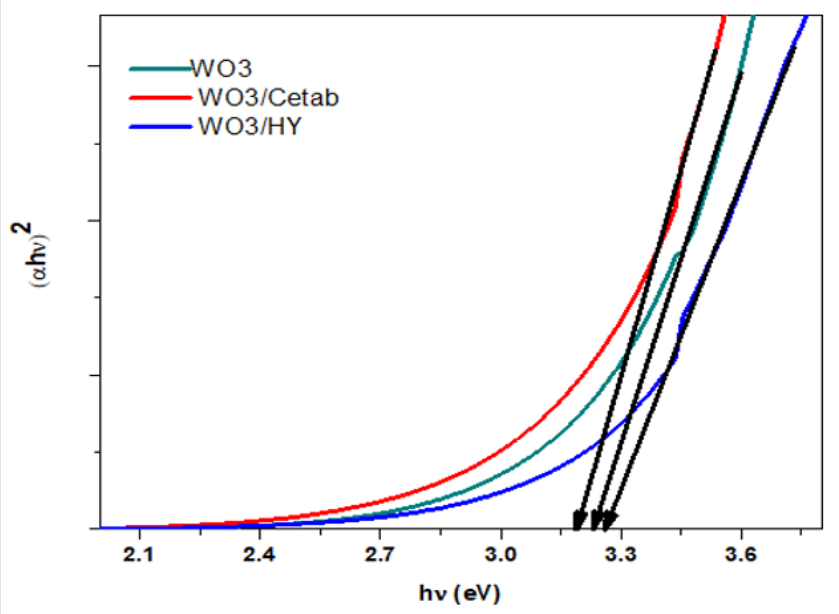

Figure 4: Optical band gap spectra of WO_3 and WO_3/ Ceteareth-25, and WO_3/HY nanoparticles.

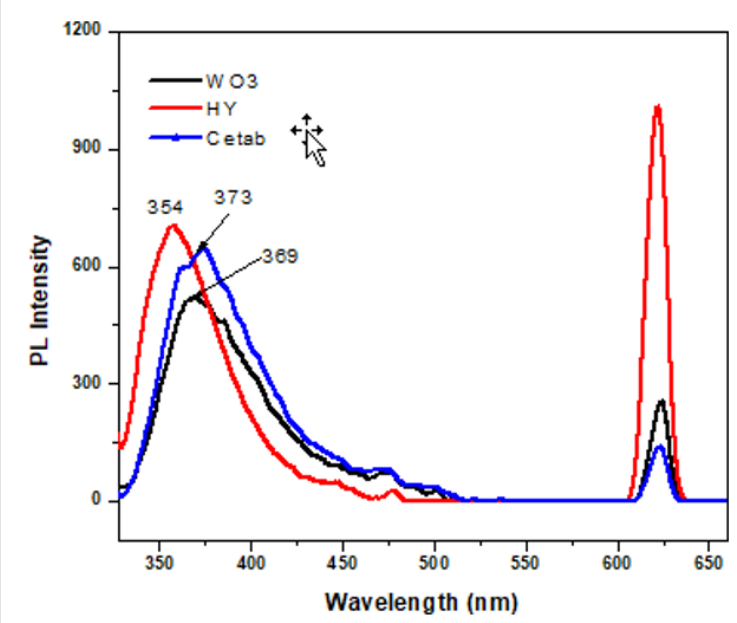

Figure 5: PL spectra of WO_3 and WO_3/ Ceteareth-25, and WO_3/HY nanoparticles.

The ultraviolet band matches the excitonic near band gap emission. The red emission peak (624nm) is associated with oxygen vacancies and these emissions can be linked to various luminescent centers, such as oxygen gaps and energy levels caused by bond hanging in nanocrystals. The PL peak position in the WO_3/ HY nanoparticles has a blue shift to lower wavelength relative to the pure WO_3 nanoparticles. The PL spectrum obtained supported our spectrum of UV absorption and showed a similar change in peak position. In comparison to pure WO_3 nanoparticles, the PL intensity of WO_3/HY nanoparticles is clearly enhanced in the visible region. Typically, different surfactant materials are used to regulate particle size as well as passivate active surface sites in the precipitation process. The quantity and composition of the surfactant determines not only the size of these materials, but also the luminescent properties. These organic additives on the nanoparticles surface reduce the number of irradiative surfaces trapping sites, resulting in an increase in PL property [42].

Conclusions

Hexagonal WO_3 nanoparticles have been synthesized using sodium tungstate dehydrate (Na_2WO_4-$2H_2O$) with additives Ceteareth-25 and alkyl hydroxyl ethyl dimethyl ammonium chloride (HY) surfactant by using precipitation method. The XRD analysis revealed that the average crystalline size was 15, 17 and 10nm, for pure WO_3, WO_3/ Ceteareth-25 and WO_3/HY nanoparticles, respectively. WO_3/HY nanoparticles showed a blue shift from the pure WO_3 nanoparticles. It is noted that, due to the formation of smaller particles, HY assisted WO_3 nanoparticles exhibit good optical properties. An increase in visible emission PL intensity was observed following surface passivation by HY surfactant.

Funding

On behalf of all authors, the corresponding author states that there is no funding for this paper

Compliance with Ethical Standards

Conflict of interest on behalf of all authors, the corresponding author states that there is no conflict of interest.

References

1. Noguera C (1996) Physics and Chemistry at Oxide Surfaces; Cambridge University Press: Cambridge, UK.
2. Kung HH (1989) Transition Metal Oxides: Surface Chemistry and Catalysis; Elsevier: Amsterdam.
3. Henrich VE, Cox PA (1994) The Surface Chemistry of Metal Oxides; Cambridge University Press: Cambridge, UK.
4. Wells AF (1987) Structural Inorganic Chemistry, 6th edn; Oxford University Press: New York, USA.
5. Rodríguez JA, Fernández-García M (Eds.) (2007) Synthesis, Properties and Applications of Oxide Nanoparticles. Whiley: New Jersey.
6. Fernández García M, Martínez-Arias A, Hanson JC, Rodríguez JA (2004) Nanostructured Oxides in Chemistry: Characterization and Properties. Chem Rev 104(9): 4063-4104.
7. Wyckoff RWG (1964) Fault-Tolerant Resolvability of Certain Crystal Structures. Crystal Structures, 2nd edn Wiley: New York, USA.
8. Gleiter H (1995) Nanostruct Mater 3: 532.
9. Valden M, Lai X, Goodman DW (1998) Onset of Catalytic Activity of Gold Clusters on Titania With the Appearance of Nonmetallic Properties. Science 281(199): 1647-1650.
10. Rodriguez JA, Liu G, Jirsak T, Hrbek Chang Z, Dvorak J (2002) Activation of Gold on Titania: Adsorption and Reaction of SO(2) on Au/TiO(2) (110). J Am Chem Soc 124(18): 5247-5250.
11. Baumer M, Freund H (1999) Metal deposits on well-ordered oxide films. J Progress in Surf Sci 61: 127-198.

12. Trudeau ML, Ying JY (1996) Nanocrystalline materials in catalysis and electrocatalysis: Structure tailoring and surface reactivity. Nanostruct Mater 7(2): 245-258.

13. Wang Z, Hu M, Qin Y (2016) Mater Lett 171: 146-149.

14. Kamali E, Ehsan H (2010) 5: 370-373.

15. Yan W, Hu M, Zeng P, Ma S, Li M (2014) A room temperature sub-ppm NO2 gas sensor based on WO3 hollow spheres. Appl Surf Sci 292: 551-555.

16. Sun S, Chang X, Li Z (2012) Mater Charact 73: 130-136.

17. Boukriba M, Sediri F, Gharbi N (2010) Theoretical and experimental vibrational spectroscopy study on rotational isomer of 4-phenylbutylamine. Polyhedron 29: 2070-2074.

18. Omri K, Bettaibi A, Khirouni K, Mir L El (2018) The optoelectronic properties and role of Cu concentration on the structural and electrical properties of Cu doped ZnO nanoparticles. Phys B Phys. Condens Matter 537: 167-175.

19. Wang X, Zhang H, Liu L, Li W, Cao P (2014) Mater Lett 130: 248-251.

20. Upadhyay SB, Mishra RK, Sahay PP (2014) Sensors Actuators B Chem 193: 19-27.

21. Kozlov DA, Shcherbakov AB, Kozlova TO, Angelov B, Kozlova TO (2020) Photochromic and Photocatalytic Properties of Ultra-Small PVP-Stabilized WO3 Nanoparticles. Molecules 25: 154.

22. Guo DZ, Yu Zhang K, Glote GM, Zhang, Xue ZQ (2004) J Mater Res 19: 3665-3670.

23. Sadakane M, Sasaki K, Kunioku H, Ohtani B, Ueda W, et al. (2008) Preparation of nano-structured crystalline tungsten(vi) oxide and enhanced photocatalytic activity for decomposition of organic compounds under visible light irradiation. Chem Commun 48: 6552-6554.

24. Mozalev AA, Khatko V, Bittencourt C, Hassel AW, Gorokh G (2008) Nanostructured Columnlike Tungsten Oxide Film by Anodizing Al/W/Ti Layers On Si. Chem Mater 20: 6482-6493.

25. Cao B, Chen J, Tang X, Zhou W (2009) Three-Dimensional Hierarchical Structure of Single Crystalline Tungsten Oxide Nanowires: Construction, Phase Transition, and Voltammetric Behavior. J Mater Chem 19: 2323-2327.

26. Zhang Y, Chen Y, Liu H, Zhou Y, Li R, et al. (2009) Phys Chem 113: 1746-1750.

27. Ashkarran AA, Irajizad A, Ahadian MM, Ardakani SAM (2008) Nanotechnology 19: 195709.

28. Lethy KJ, Beena D, MahadevanPillai VP, Ganesan V (2008) Bandgap renormalization in titania modified nanostructured tungsten oxide thin films prepared by pulsed laser deposition technique for solar cell applications. J Appl Phys (104-3): 033515-12.

29. Rajagopal S, Nataraj D, Mangalaraj D (2009) Nanoscale Res Lett 4: 1335-1342.

30. Priya R, Sethu Raman M, Senthilkumar N, Balan R, International Journal of Science and Research (IJSR), ISSN (Online): 2319-7064.

31. Hariharan V, Aroulmoji V, Sekar C, Shanthakumar A, Kumara Dhas M (2016) Int J Adv Sci Eng 3: 299-307.

32. Sheifali Shukla, Savita Chaudhary, Ahmad Umar, Ganga Ram Chaudhary, Sushil Kumar Kansal (2016) Chemical Engineering Journal 288: 423-431.

33. Chai Yan Ng, Khairunisak Abdul Razak, Azlan Abdul Aziz, ZainoviaLockman (2014) Journal of Experimental Nanoscience 9: 9-16.

34. Toberer ES, Seshadri R (2006) Template-free routes to porous inorganic materials. Chem Commun (Camb) 30: 3159.

35. Xintai Su, Feng Xiao, Yani Li, JikangJian, Qingjun Sun (2010) Synthesis and Optical Properties of Colloidal Tungsten Oxide Nanorods. Materials Letters 64: 1232-1234.

36. Shukla S, Chaudhary S, Umar A, Chaudhar GR, Kumar Kansal S (2016) Chemical Engineering Journal 288: 423-431

37. Salem J, Hammad T, Harrison R (2009) Zno Nanoparticles Prepared in The Presence of Additives by Thermal Decomposition Method. Int J Nanosci 8: 465-472.

38. Hammad TM, Salem JK, Harrison RG (2009) Rev Adv Mater Sci 22: 74-80.

39. Benzitouni S (2017) Int J Light Electron Opt.

40. Mohammadi S, Sohrabi M, Golikand AN, Fakhri A (2016) Photodegradation of 4-nitrophenol over B-doped TiO2 nanostructure: effect of dopant concentration, kinetics, and mechanism. J Photochem Photobiol B Biol 161: 217–221.

41. Ramkumar S, Rajarajan G (2016) One-step microwave synthesis of pure and Mn doped WO_3 nanoparticles and its structural, optical and electrochemical properties. J Mater Sci 27: 1847-1853.

42. Talaat M, Hammad, Jamil K Salem, Kuhn S, Mohammed Abu Draaz, et al. (2015) Optical properties of Cu2+ and Fe2+ doped ZnS semiconductor nanoparticles synthesized by coprecipitation method. Mater Sci: Mater Electron 26: 5495-5501.

ISSN: 2574-1241

DOI: 10.26717/BJSTR.2020.28.004701

Fawzi S Kodeh. Biomed J Sci & Tech Res